Journal of Robotics and Control (JRC)
Volume 6, Issue 3, 2025
ISSN: 2715-5072, DOI: 10.18196/jrc.v6i3.26324

Optimizing Input Shaping for Flexible Beam Vibration Control Using Self-Adaptive Differential Evolution

Phuong-Tung Pham [1], Thanh Huy Phung [2], Quoc Chi Nguyen [3*]
[1, 2, 3] Department of Mechatronics, Faculty of Mechanical Engineering, Ho Chi Minh City University of Technology (HCMUT), 268 Ly Thuong Kiet Street, District 10, Ho Chi Minh City, Vietnam
[1, 2, 3] Vietnam National University Ho Chi Minh City, Linh Trung Ward, Thu Duc City, Ho Chi Minh City, Vietnam
Email: [1] pptung@hcmut.edu.vn, [2] huypt@hcmut.edu.vn, [3] nqchi@hcmut.edu.vn
*Corresponding Author

***Abstract*—This study develops a control strategy for the flexible beam linked to a moving hub utilizing input shaping control. The input shaping control technique is an open-loop control approach that employs a shaped command to suppress the undesired vibration. This command is formed by convolving the original command with input shapers (a sequence of impulses with amplitude and temporal location). Unlike the conventional input shaping control, which calculates the input shapers based on the system's natural frequencies and attenuation ratios, a metaheuristic input shaper searcher based on the self-adaptive differential evolution algorithm is employed in this paper to identify the optimal input shapers. Using this algorithm, the specifications of input shapers, including the amplitudes and time locations, can be optimized to ensure that the cost function corresponding to the position error and beam's vibration approaches the global minimum value. The control performance is proved via the numerical simulation. The simulation results demonstrate that input shaping control utilizing optimized input shapers can significantly reduce residual vibrations in the beam. While this control strategy requires substantial computational resources and longer computation times to develop the optimal input shapers compared to traditional techniques, the effectiveness of the optimal input shapers in attenuating vibrations is remarkable.**

***Keywords*—Flexible Cantilever Beam; Input Shaping Control; Self-Adaptive Differential Evolution; Vibration Control; JADE.**

I. INTRODUCTION

Automobile engineering frequently uses systems with a cantilever beam connected to a moving hub. Examples of such systems include CNC EDM (electrical discharge machining) drilling machines [1], gantry manipulators [2], and cartesian palletizers [3] (Fig. 1). A cantilever beam may be either rigid or flexible, depending on its stiffness and the specific aspect under consideration. The Cartesian palletizer with a lightweight arm can be represented as a flexible cantilever beam for the robotic arm, while the trolley is seen as a translating hub. During the placement operation, the trolley's movement induces undesirable transverse vibrations in the robotic arm. This undesirable vibration is a factor constraining the machine's productivity. Therefore, this undesirable vibration must be mitigated.

A flexible beam linked to a moving hub comprises two primary elements: the beam and the hub. The dynamic model of an elastic beam, represented by the Euler-Bernoulli beam theory, is defined by a partial differential equation (PDE) [4]-[13]. Conversely, the governing equation of the hub is an ordinary differential equation (ODE). Furthermore, if a payload is attached to the beam's tip, the payload dynamic will be described by another ODE. Dynamic models of the beam-hub system have been established in the literature [14]-[20]. As a result, the hub's movement influences the dynamics of the beam's vibration and vice versa. The vibration control of a flexible beam mounted on a rigid moving base has been the subject of extensive research [5], [21]-[23]. He et al. [21] dealt with the vibration control of a rigid-flexible wing system. Additionally, Pham et al. [14], [22] explored the boundary control challenges associated with a flexible beam in three-dimensional space, examining two distinct scenarios: one involving a beam of constant length and the other featuring a beam with variable length. Most research on flexible beams typically employs the Euler-Bernoulli beam theory to model the beam. Some studies further expand this by utilizing Timoshenko beam theory [24]-[26]. In [24], the authors modeled a flexible beam clamped to a rigid rectilinearly mobile frame on an elastic foundation using the Timoshenko beam theory. According to this model, a discrete-time sliding mode controller is designed for tracking control and vibration suppression in the presence of actuator bandwidth limitation and control input saturation.

Vibration suppression of flexible beams can be executed via feedback control methodologies [27]-[44]. Displacement data from multiple points on the beam is obtained using sensors, including strain gauges or lasers. The control signal is created and applied to actuators based on the feedback signals. Despite its effectiveness in suppressing vibrations in flexible beams, the feedback control approach has drawbacks. Installing sensors on beams is a significant challenge in certain circumstances. Feed-forward control techniques, including input shaping control, may be implemented in these situations [45]-[57]. Input shaping control is a method that employs a suitably designed command signal to reduce the residual vibrations of the beam. This approach has been used for many vibrational issues, including overhead cranes [58], [59], MEMS [60], [61], and spacecraft [62]. Shah and Hong [63] employed input shaping control to mitigate vibrations in an underwater flexible beam mounted to a moving trolley, while Pham et al. [64] performed an experimental investigation to validate the efficacy of various input shaping control methods. The shaped command signal is fundamental to input shaping control. Generating an appropriate command signal is essential for enhancing control efficacy. From an engineering perspective, input shaping control shows that a shaped command signal can reduce the system's vibration. The traditional methodology considers the flexible beam a single-mode system represented by a second-order harmonic oscillator model. The input shapers are established according to this second-order harmonic oscillator's natural frequency and damping ratio. However, the flexible beam is a system with an infinity vibrational mode. The expected control efficiency might not be attained if the system is assumed to have only one or two modes. The input shaping controller exhibits high sensitivity to the estimated error in natural frequency and damping ratio. Therefore, the natural frequency and damping ratio must be carefully estimated to achieve high control performance. To overcome this problem, we can establish an optimization problem by finding the best-shaped command signal for minimizing the vibrational energy of the system.

The optimization problem can be addressed utilizing a metaheuristic algorithm, namely the Differential Evolution (DE) algorithm [65]-[77]. Differential evolution is a subset of evolutionary algorithms derived from the natural evolution of species. This algorithm was initially presented by Storn and Price [78]. The primary advantages of this algorithm are its ease of implementation and favorable convergence characteristics. Owing to these advantages, it is becoming increasingly popular and extensively utilized across various issues [79]. The DE algorithm has been utilized in vibration control to optimize the controller control settings. Saad et al. [80] developed a closed-loop control method for a flexible beam utilizing PID control. The authors employed the DE method to optimize the tuning of the PID controller for effective vibration suppression. Marinakis et al. [81] created a fuzzy control system to suppress vibrations in smart structures, with the parameters of the fuzzy control system tuned by differential evolution (DE). Given the advantages of differential evolution, it is evident that DE is a good approach for optimizing active vibration control.

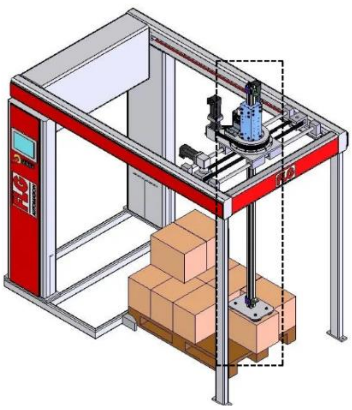

Fig. 1. Linear palletizer (www.medicalexpo.com/prod/flg-automation-ag/product-111920-974512.html)

To the best of the authors' knowledge, the majority of studies exploring the application of JADE for vibration control in flexible beams have predominantly centered on feedback controllers. However, it is essential to recognize that feedforward controllers, such as input shaping, possess distinct advantages of their own. This study proposes a control strategy for a flexible beam connected to a moving hub, employing input shaping control to effectively mitigate undesirable vibrations. The proposed approach uses a metaheuristic search based on a self-adaptive differential evolution algorithm to identify and optimize input shapers' properties—specifically their amplitudes and time locations—minimizing the cost function related to position error and beam vibrations. Numerical simulations are conducted to validate the effectiveness of the proposed control scheme. The main contribution of this study is to propose an optimization method for the input shaping controller for a flexible cantilever beam system attached to a moving base based on self-adaptive differential evolution algorithm.

The remainder of this paper is organized as follows: Section 2 introduces methodologies, including the input shaping control and metaheuristic shaper search scheme. Section 3 develops the dynamic model essential for the search scheme. Section 4 shows the simulation results, whereas Section 5 gives some conclusions.

II. METHODOLOGIES

A. Input Shaping Control

The control objectives of the beam-hub system (i.e., Fig. 2) are to position the hub at a designated location yd and to eliminate the beam's vibrations using a control force f. While relocating the hub to a specified position can be executed via a PD controller, expressed as $f = K_P.y + K_D(dy/dt)$, suppressing the beam's vibration is conducted by integrating the input shaping control technique with the PD controller.

The input shaping control technique produces a shaped command by convolving the original command with input shapers, which are defined as a sequence of impulses characterized by amplitude A_i and time location t_i (refer to Fig. 3). Appropriate input shapers can significantly suppress vibration when utilizing the shaped command. Identifying the input shapers to implement the input shaping technique is essential [82].

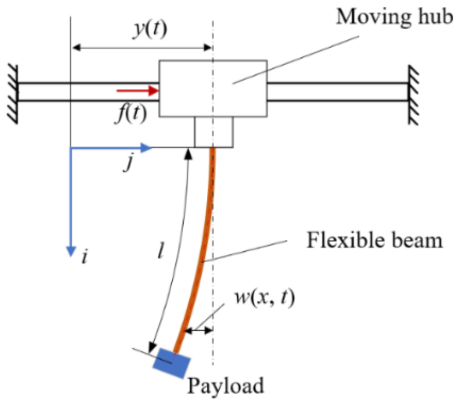

Fig. 2. System of a flexible beam attached to a moving hub

B. Metaheuristic Input Shaper Search Scheme

This paper introduces a novel control scheme for a flexible beam attached to a moving base. The optimum input shapers are determined using a metaheuristic technique. Fig. 4 illustrates the control scheme. The mathematical model of the actual system is initially established using data-driven or physics-based methods. The computer solves the optimization problem, which involves tuning and selecting the control parameters and the optimal input shapers (i.e., determining the amplitude and time location, A_i and t_i) to minimize the discrepancy between the system response and the desired response, according to a developed mathematical model. After that, the optimal input shapers are implemented in the actual system. The optimization problem can be summarized as follows:

Find the vectors of the amplitude and time location of input shapers, i.e., $A_{IS} = [A_1, A_2, \dots, A_M]$ and $T_{IS} = [t_1, t_2, \dots, t_M]$, where M is the number of the input shapers, and the control parameter K_P and K_D, such that the following objective function is minimized.

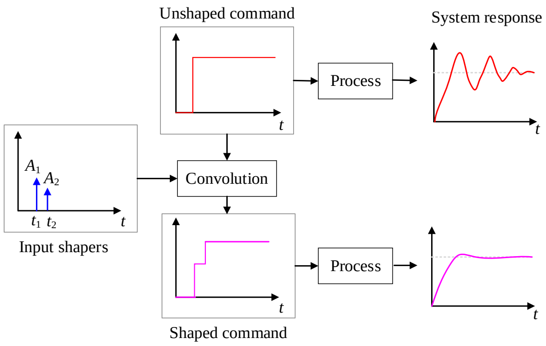

Fig. 3. Input shaping control

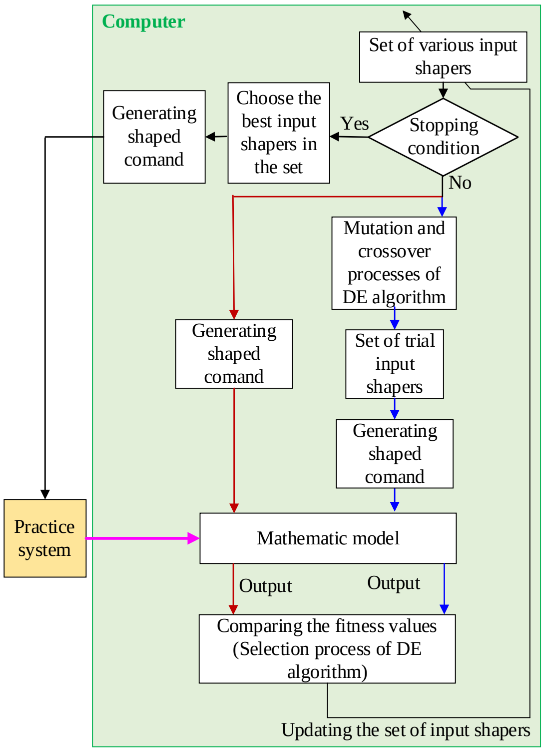

Fig. 4. The control scheme is based on input shaping and differential evolution methods

$$F_{\text{Obj}} = \int_0^t e^{\vartheta t}[y(t) + w(l,t)]^2 dt, \tag{1}$$

where $\vartheta = 0.2$ is the weighting factor.

C. Self-Adaptive Differential Evolution Algorithm

A self-adaptive differential evolution algorithm, JADE, is employed to resolve the optimization problem in the proposed scheme [83]-[91]. The concept of differential evolution is based on the species evolution theory. Each candidate solution of the optimization problem, $x = [A_1, A_2, \dots, A_M, t_1, t_2, \dots, t_M, K_D, K_P]$, is considered an individual. A population $\boldsymbol{P}$, consisting of N individuals, is generated randomly for the first generation. Population P will undergo mutation, crossover, and selection processes to meet the minimum requirements of the objective function. This continuous process occurs over multiple generations, allowing individuals within population P to progressively enhance their performance, ultimately enabling them to minimize the objective function effectively. The efficacy and effectiveness of the algorithm are significantly influenced by two parameters in DE: F (scale factor) during the mutation phase and Cr (crossover rate) during the crossover phase. Cr maintains the equilibrium between exploration and exploitation in the search space, whereas F affects convergence speed. It is imperative to tune these parameters appropriately to achieve optimal performance in particular optimization problems. The conventional DE involves manual tuning of these parameters. A variant of the DE, called JADE, was introduced to enhance DE. The scale factor and crossover rate in JADE are self-adaptive, enabling the algorithm to dynamically modify and learn about them during optimization. In addition, JADE introduces the "*current-to-p-best*" strategy [83], which involves the mutant vector being influenced by the best solutions in addition to random vectors. This helps balance exploration and exploitation.

In this problem, the j-th individual in the population of the G-th generation is shown as follows.

$$\mathbf{x}_j^G = [x_{1,j}^G, x_{2,j}^G, x_{3,j}^G, \dots, x_{(2M+2),j}^G] \tag{2}$$

For each generation, each individual in the population is selected as a parent vector. Each parent vector undergoes an evolution process, including the mutation, crossover, and selection steps.

Mutation: A mutant vector $\mathbf{m}_j^G = [m_{1,j}^G, m_{2,j}^G, m_{3,j}^G, \dots, m_{(2M+2),j}^G]$ is generated corresponding to the parent vector $\mathbf{x}_j^G$ via the following formula.

$$\mathbf{m}_j^G = \mathbf{x}_j^G + F_j(\mathbf{x}_a^G - \mathbf{x}_b^G) + F_j(\mathbf{x}_{\text{best}}^G - \mathbf{x}_j^G), \tag{3}$$

where $\mathbf{x}_a^G$ and $\mathbf{x}_b^G$ are distinct individuals selected randomly from the population, additionally, $a, b \neq j$; F_j is the scaling factor of each individual $\mathbf{x}_j^G$, $F_j \in [0,1]$. The scale factor F_j is independently generated according to the Cauchy distribution with location parameter μ_F and standard deviation parameter 0.1, namely,

$$F_j = \mathrm{randc}_j(\mu_F, 0.1). \tag{4}$$

The location parameter μ_F of the Cauchy distribution is initially set to 0.5 and subsequently updated at the conclusion of each generation:

$$\mu_F = (1-\delta)\cdot\mu_F + \delta\cdot\mathrm{mean}_L(S_F), \tag{5}$$

where δ is the learning rate $c \in [0,1]$, S_F denotes the set of all successful mutation factors in the G-th generation, and $mean_L(\cdot)$ is the Lehmer mean.

Crossover: A trial vector $\mathbf{u}_j^G = [u_{1,j}^G, u_{2,j}^G, u_{3,j}^G, \ldots, u_{(2M+2),j}^G]$ is determined based on the crossover of the parent vector $\mathbf{x}_j^G$ and the mutant vector $\mathbf{m}_j^G$. The i-th element of $\mathbf{u}_j^G$ has a $Cr \times 100\%$ chance of getting the value of the corresponding element of $\mathbf{m}_j^G$; otherwise, it gets the value of the i-th element of $\mathbf{x}_j^G$.

$$u_{i,j}^G = \begin{cases} m_{i,j}^G & \text{if } rand(0,1) \le Cr, \\ x_{i,j}^G & \text{otherwise} \end{cases} \tag{6}$$

where Cr is the crossover probability, which is generated based on normal distribution of mean μ_{Cr} and standard deviation parameter 0.1, i.e.,

$$Cr_j = \mathrm{randn}_j(\mu_{Cr}, 0.1), \tag{7}$$

$$\mu_{Cr} = (1-\delta)\cdot\mu_{Cr} + \delta\cdot\mathrm{mean}_A(S_{Cr}), \tag{8}$$

where S_{Cr} denotes the set of all successful crossover probabilities in G-th generation, and $mean_A(\cdot)$ is the usual arithmetic mean.

Selection: The fitness value of the trial vector $\mathbf{u}_j^G$is compared with one of the parent vector $\mathbf{x}_j^G$. The one with worse fitness is eliminated, whereas the remaining one survives to the next generation.

$$\mathbf{x}_j^{G+1} = \begin{cases} \mathbf{u}_j^G & \text{if } F_{\mathrm{Obj}}(\mathbf{u}_j^G) \le F_{\mathrm{Obj}}(\mathbf{x}_j^G), \\ \mathbf{x}_j^G & \text{otherwise.} \end{cases} \tag{9}$$

Through these steps, the good individuals are retained in the population, whereas the flawed individuals are replaced by the better ones (i.e., those with better fitness values). The evolution process is repeated, and the population gets better and better with each generation. When a predefined termination criterion is satisfied, the evolution stops, and the individuals of the current generation can be chosen as the solution to the optimal problem.

The self-adaptive nature of the JADE algorithm, while offering significant adaptability and optimization capabilities, presents certain drawbacks. A primary concern is the risk of premature convergence, where the algorithm may stop exploring potential solutions too early and settle on a suboptimal result. This hinders the identification of better solutions that may exist outside the current search area.

Additionally, the algorithm's performance can diminish in high-dimensional search spaces, which often contain multiple local optima. As dimensionality increases, maintaining diversity among candidate solutions becomes challenging, further exacerbating the likelihood of premature convergence.

To mitigate these issues, it is crucial to incorporate strategies that enhance exploration, such as maintaining a diverse population of solutions or employing multi-objective optimization techniques.

III. DYNAMIC MODEL

As shown in Fig. 3, the dynamic model of the beam-base system is essential for tuning the input shaping controller. This system consists of a flexible beam of length l, which is securely clamped to a translating base with mass m, as illustrated in Fig. 2. beam can be used to modeling the beam. In this research, assuming that the beam is both elastic and uniform. Furthermore, it is postulated that the cross-sections of the beam remain planar and perpendicular to the beam's axis following deformation, thereby neglecting shear deformations. Consequently, the Euler-Bernoulli beam theory is employed for modeling the beam. A payload, also with mass m_p, is attached to the tip of the beam. In Fig. 2, $w(x,t)$ represents the transverse vibrations of the beam, while $y(t)$ indicates the position of the base. The mass density ρ defines the beam's properties, Young's modulus E, the first moment of area I, and the cross-sectional area A. The system's kinematic and potential energies and work done can be described, respectively, as follows:

$$K = \frac{1}{2}\rho A\int_0^l (\dot{y}+w_t)^2 dx + \frac{1}{2}M\dot{y}^2 + \frac{1}{2}m_p(\dot{y}+w_t)^2|_{x=l}, \tag{10}$$

$$U = \frac{1}{2}\int_0^l P(x,t){w_x}^2 dx + \frac{1}{8}\int_0^l EA{w_x}^4 dx + \frac{1}{2}\int_0^l EI{w_{xx}}^2 dx, \tag{11}$$

$$\delta W = f\delta y - c\int_0^l {w_t}^2 \delta w dx, \tag{12}$$

where $P(x,t) = \rho A(l-x)g$ is the axial force generated by the gravitational acceleration g. In this study, w_t and w_x indicate the partial derivative of $w(x,t)$ concerning t and x, respectively, whereas $\dot{y}$ is the total derivative of $y(t)$. According to Halminton's principle,

$$\int_{t_1}^{t_2}(\delta K - \delta U + \delta W)dt = 0, \tag{13}$$

the dynamic model for the considered system can be developed as follows

$$\rho A(\ddot{y}+w_{tt}) + cw_t - P_x w_x - P w_{xx} - \frac{3}{2}EA w_{xx}{w_x}^2 + EI w_{xxxx} = 0, \tag{14}$$

with boundary conditions:

$$w(0,t) = 0,\ \frac{\partial w(0,t)}{\partial x} = 0, \tag{15}$$

$$m_p(\ddot{y} + w_{tt}(l,t)) + EA(w_x(l,t))^3/2 - EIw_{xxx}(l,t) = 0, \quad (16)$$

$$M\ddot{y} - c\int_0^l w_x dx + EIw_{xxx}(0,t) = f, \quad (17)$$

IV. NUMERICAL SIMULATIONS

The objective of this numerical simulation is to verify the efficiency of the control system that was developed in the previous sections. The control target is to move the payload to a desired position y_d and minimize its vibration. MATLAB is employed to execute simulation. The approximate solutions for the equations of motion are determined using the finite difference method, wherein the time step is Δt = 0.0001, and the space step is Δx = 0.04.

The metaheuristic input shaper search scheme shown in Fig. 4 is used to determine the amplitude and time location vectors of input shapers, i.e.,

$$\begin{bmatrix} A_{IS} \\ t_{IS} \end{bmatrix} = \begin{bmatrix} A_1 & A_2 & A_3 & A_5 & A_5 \\ 0 & t_2 & t_3 & t_4 & t_5 \end{bmatrix}, \quad (18)$$

where the amplitude vector is constrained by condition: $A_1 + A_2 + A_3 + A_4 + A_5 = 1$.

System parameters used in numerical simulation are shown in Table I, whereas the parameters for JADE are introduced in Table II. It is noted that the individual in the JADE algorithm is an 11-dimensional vector, i.e.,

$$\mathbf{x} = [A_1, A_2, A_3, A_4, A_5, t_2, t_3, t_4, t_5, K_P, K_D]. \quad (19)$$

Fig. 5 illustrates the convergence profile of the seft-adaptivelf differential evolution method. A minimal value of F_{Obj} is reached by the fitness of 50 individuals in the population after 95 generations. The optimum values for control parameters, the shaper's amplitudes, and the time location are shown as follows:

$$[K_P \quad K_D] = [185.16 \quad 166.21] \quad (20)$$

$$[A_{IS} \quad t_{IS}] = \begin{bmatrix} 0.2533 & 0 \\ 0.7093 & 0.008 \\ 0.0095 & 1.0666 \\ 0.0010 & 1.1171 \\ 0.0269 & 2.0335 \end{bmatrix}. \quad (20)$$

Fig. 6 depicts the system response for three scenarios: an unshaped command signal, an optimally shaped command, and a conventionally shaped command. The conventional command utilizes a zero-vibration shaper created based on the system's approximate natural frequency and damping ratio. The optimal command signal effectively and rapidly suppresses residual vibrations in the system, as illustrated in Fig. 6. A direct comparison of the response of conventional input shaping control with that of the proposed input shaper reveals that the latter offers significantly enhanced control performance. Additionally, Fig. 7 demonstrates the vibration of the payload in detail, whereas Fig. 8 shows the vibration along the beam.

TABLE I. SYSTEM PARAMETERS

Parameter	Value	Unit
ρ	2700	kg/m^3
E	70×10^9	N/m^2
A	6×10^{-5}	m^2
I	1.25×10^{-10}	m^4
l	0.4	m
M	10	kg
m_p	2	kg
c	0.001	Ns/m
y_d	0.4	m

TABLE II. PARAMETERS OF JADE

Parameter	Value
Dimension of the individual	11
Population size N	50
Maximum generation G_{max}	100
Initial value of μ_F	0.5
Initial value of μ_{Cr}	0.5
Learning rate δ	0.08

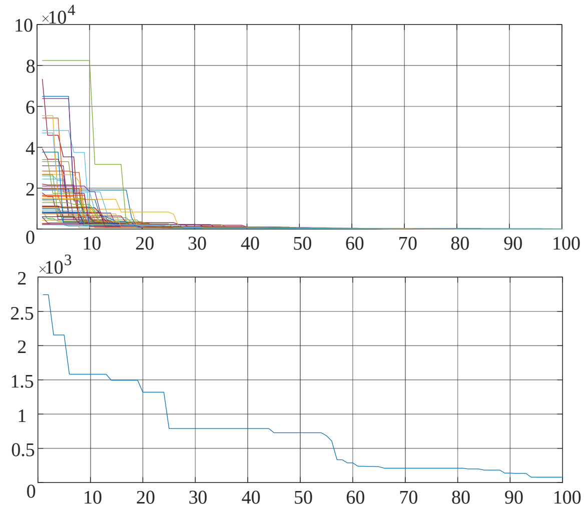

Fig. 5. Convergence profile of the DE of (a) 50 individuals and (b) the first individual

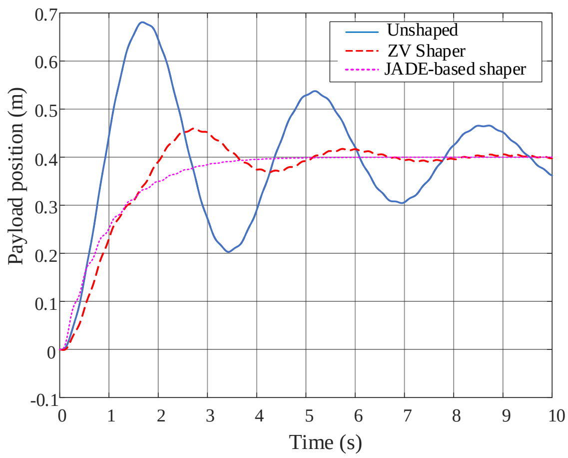

Fig. 6. Response of the payload position (i.e., $y(t) + w(l,t)$)

The sensitivity analysis has been included in the study. The simulation results show that the system remains robust despite modeling errors. The controller was developed using the model parameters listed in Table I. Even with variations in system parameters, the controller consistently performs well in suppressing vibrations. Fig. 9 presents the results for actual payload masses of 2, 3, 4, and 5 kg, while the controller is based on a payload mass of 2 kg. Additionally, Fig. 10 illustrates the controller's robustness when there are errors in the material properties of the beam during the modeling process.

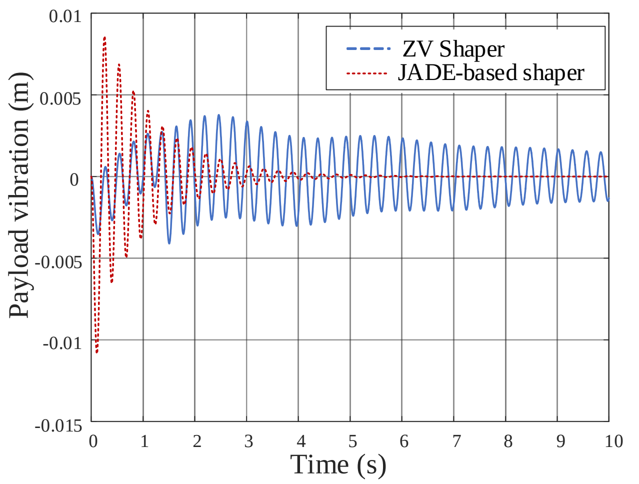

Fig. 7. Vibration of the payload $w(l,t)$

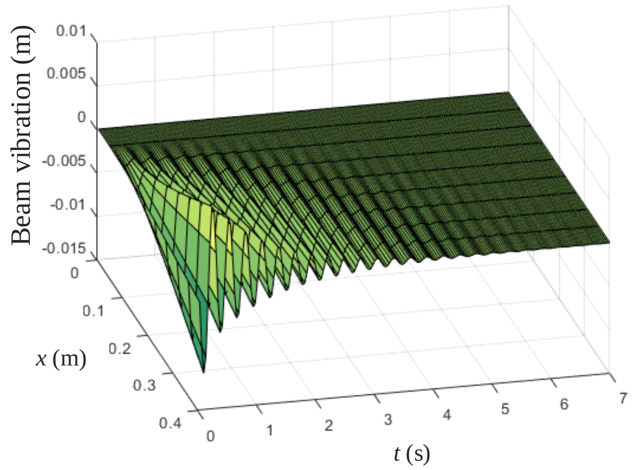

Fig. 8. Vibration of the beam $w(x,t)$

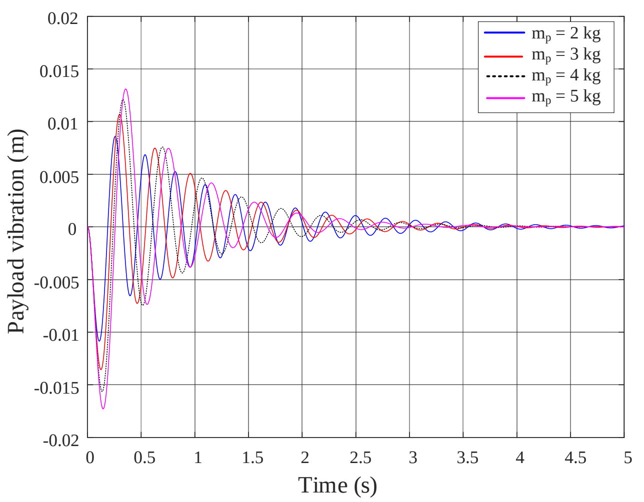

Fig. 9. Robustness of the proposed controller under the variation of the payload mass

Additionally, a comparison of the effectiveness of the proposed controller with a feedback-based controller utilized in previous studies [27][14] is conducted. The results presented in Fig. 11 indicate that the control performance of both controllers is quite similar. While the feedback controller demonstrates a slightly improved control effectiveness, the proposed control law also exhibits commendable performance. Notably, the developed controller does not rely on feedback sensors for measuring beam deformation when calculating the control force.

The simulation results underscore the effectiveness of JADE in designing input shapers, demonstrating that JADE-based input shapers can efficiently eliminate unwanted vibrations.

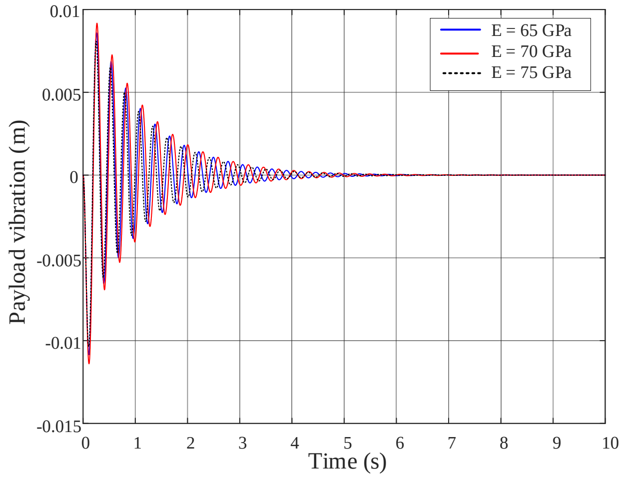

Fig. 10. Robustness of the proposed controller under the variation of the material properties

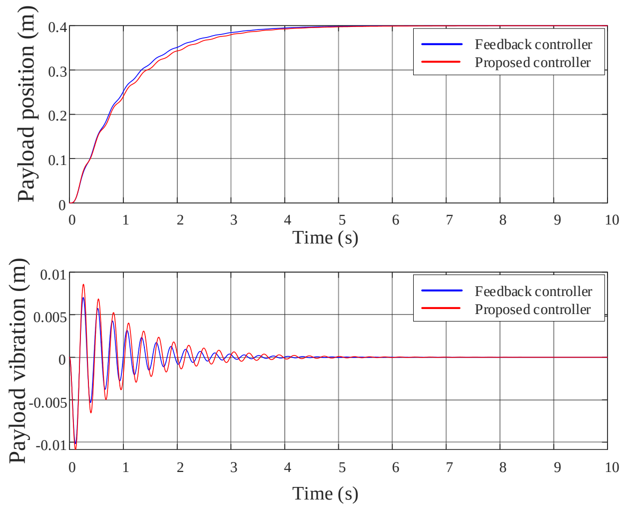

Fig. 11. Comparision of the proposed controller with the feedback control

While this control solution demands complex computational capabilities, which may present challenges for its implementation in industrial settings, it is important to note that in automated production lines, the structures and system parameters generally do not change significantly over extended periods. Consequently, it is adequate to employ the algorithm for calculating the shapers only during the system's calibration phase, thereby alleviating the need for continuous complex computations throughout the operational lifetime of the machinery. Furthermore, implementing the proposed control method in practical scenarios presents challenges such as the need for high-precision sensors, as inaccuracies from sensor noise or calibration errors can lead to ineffective control decisions and positioning errors. Additionally, external disturbances like environmental noise and friction can significantly impact control performance and stability.

V. Conclusions

A control scheme for the flexible translating beam with a payload was proposed in this paper, which employs the input shaping control technique. This work employs a metaheuristic input shaper search methodology utilizing a self-adaptive differential evolution algorithm, unlike traditional input shaping control, which computes input shapers based on natural frequency and damping ratio. The proposed control technique autonomously identifies the optimal input shaper to reduce the position error of the payload. The efficacy of the proposed control strategy is validated by simulation. The command signal generated by the optimal input shapers guarantees that the payload reaches the target position while minimizing oscillation rapidly.

In addition, the proposed control strategy has certain limitations related to modeling. While the simulation results indicate that the controller is robust against variations in model parameters, creating a mathematical model for complex systems presents a considerable challenge. Moreover, the issue of computational complexity is another factor that restricts the practical application of the proposed algorithm.

In the future, experimental research should be conducted to validate the robustness of the controller against uncertainties encountered during actual operational conditions. Additionally, exploring the application of the algorithm to more complex systems, such as flexible beams with variable lengths, presents another avenue for future research.

Acknowledgment

This research is funded by Ho Chi Minh City University of Technology (HCMUT), VNU-HCM under grant number To-CK-2023-01. We acknowledge Ho Chi Minh City University of Technology (HCMUT), VNU-HCM for supporting this study.

References

[1] W. Xia, Z. Li, M. Chen, Y. Zhang, and W. Zhao, “Study on electrode vibration in the touch-down stage of fast electrical discharge machining drilling,” *Int. J. Adv. Manuf. Technol.*, vol. 109, pp. 2273–2283, 2020.

[2] B. Li, X. Li, H. Gao, and F. -Y. Wang, "Advances in Flexible Robotic Manipulator Systems — Part II: Planning, Control, Applications, and Perspectives," in *IEEE/ASME Transactions on Mechatronics*, vol. 29, no. 3, pp. 1680-1689, June 2024.

[3] A. Beiranvand, A. Kalhor, and M. T. Masouleh, “Modeling, identification and minimum length integral sliding mode control of a 3-DOF cartesian parallel robot by considering virtual flexible links,” *Mech. Mach. Theory*, vol. 157, p. 104183, 2021.

[4] B. Li, X. Li, H. Gao, and F. -Y. Wang, "Advances in Flexible Robotic Manipulator Systems—Part I: Overview and Dynamics Modeling Methods," in *IEEE/ASME Transactions on Mechatronics*, vol. 29, no. 2, pp. 1100-1110, April 2024.

[5] W. Hu, M. Xu, F. Zhang, C. Xiao, and Z. Deng, “Dynamic analysis on flexible hub-beam with step-variable cross-section,” *Mech. Syst. Signal Process.*, vol. 180, p. 109423, 2022.

[6] A. Öchsner and A. Öchsner, “Euler–Bernoulli beam theory,” *Class. Beam Theor. Struct. Mech.*, pp. 7–66, 2021.

[7] J. A. Haider, F. Zaman, S. A. Lone, S. Anwar, S. A. Almutlak, and I. E. Elseesy, “Exact solutions of Euler–Bernoulli beams,” *Mod. Phys. Lett. B*, vol. 37, no. 33, p. 2350161, 2023.

[8] L. Wang, Y. Chen, G. Cheng, and T. Barrière, “Numerical analysis of fractional partial differential equations applied to polymeric visco-elastic Euler-Bernoulli beam under quasi-static loads,” *Chaos Solitons Fractals*, vol. 140, p. 110255, 2020.

[9] G. Zhang and X.-L. Gao, “A new Bernoulli–Euler beam model based on a reformulated strain gradient elasticity theory,” *Math. Mech. Solids*, vol. 25, no. 3, pp. 630–643, 2020.

[10] G. Snehasagar, C. Krishnanunni, and B. Rao, “Dynamics of vehicle–pavement system based on a viscoelastic Euler–Bernoulli beam model,” *Int. J. Pavement Eng.*, vol. 21, no. 13, pp. 1669–1682, 2020.

[11] X. Zhang, D. Thompson, and X. Sheng, “Differences between Euler-Bernoulli and Timoshenko beam formulations for calculating the effects of moving loads on a periodically supported beam,” *J. Sound Vib.*, vol. 481, p. 115432, 2020.

[12] A. M. Ahmed and A. M. Rifai, “Euler-bernoulli and timoshenko beam theories analytical and numerical comprehensive revision,” *Eur. J. Eng. Technol. Res.*, vol. 6, no. 7, pp. 20–32, 2021.

[13] P.-T. Pham and K.-S. Hong, “Dynamic models of axially moving systems: A review,” *Nonlinear Dyn.*, vol. 100, no. 1, pp. 315–349, 2020.

[14] P.-T. Pham, Q. C. Nguyen, M. Yoon, and K.-S. Hong, “Vibration control of a nonlinear cantilever beam operating in the 3D space,” *Sci. Rep.*, vol. 12, no. 1, p. 13811, 2022.

[15] X. Guo, X. Yang, F. Liu, Z. Liu, and X. Tang, “Dynamic analysis of the flexible hub-beam system based on rigid-flexible coupling mechanism,” *Proc. Inst. Mech. Eng. Part K J. Multi-Body Dyn.*, vol. 234, no. 3, pp. 536–545, 2020.

[16] L. Kloda and J. Warminski, “Nonlinear longitudinal–bending–twisting vibrations of extensible slowly rotating beam with tip mass,” *Int. J. Mech. Sci.*, vol. 220, p. 107153, 2022.

[17] M. Xu, W. Hu, Z. Han, H. Bai, Z. Deng, and C. Zhang, “Symmetry-breaking dynamics of a flexible hub-beam system rotating around an eccentric axis,” *Mech. Syst. Signal Process.*, vol. 222, p. 111757, 2025.

[18] J. Fan, D. Zhang, and H. Shen, “Dynamic modeling and simulation of a rotating flexible hub-beam based on different discretization methods of deformation fields,” *Arch. Appl. Mech.*, vol. 90, pp. 291–304, 2020.

[19] W. Hu *et al.*, “Mechanoelectrical flexible hub-beam model of ionic-type solvent-free nanofluids,” *Mech. Syst. Signal Process.*, vol. 159, p. 107833, 2021.

[20] J. Warminski, L. Kloda, and S. Lenci, “Nonlinear vibrations of an extensional beam with tip mass in slewing motion,” *Meccanica*, vol. 55, no. 12, pp. 2311–2335, 2020.

[21] W. He, T. Wang, X. He, L.-J. Yang, and O. Kaynak, “Dynamical modeling and boundary vibration control of a rigid-flexible wing system,” *IEEEASME Trans. Mechatron.*, vol. 25, no. 6, pp. 2711–2721, 2020.

[22] P.-T. Pham, Q. C. Nguyen, J. Kwon, and K.-S. Hong, “Adaptive control of a flexible varying-length beam with a translating base in the 3d space,” *Int. J. Control Autom. Syst.*, vol. 21, no. 3, pp. 711–726, 2023.

[23] Y. Wang, Y. Fang, L. Li, D. Zhang, W.-H. Liao, and J. Fang, “Dynamic modeling and vibration suppression of a rotating flexible beam with segmented active constrained layer damping treatment,” *Aerospace*, vol. 10, no. 12, p. 1010, 2023.

[24] M. R. Homaeinezhad and M. Abbasi Gavari, “Feedback control of actuation-constrained moving structure carrying Timoshenko beam,” *Int. J. Robust Nonlinear Control*, vol. 33, no. 3, pp. 1785–1806, 2023.

[25] P.-T. Pham, G.-H. Kim, and K.-S. Hong, “Vibration control of a Timoshenko cantilever beam with varying length,” *Int. J. Control Autom. Syst.*, vol. 20, no. 1, pp. 175–183, 2022.

[26] M. Vakil, E. Sharbati, A. Vakil, F. Heidari, and R. Fotouhi, “Vibration analysis of a Timoshenko beam on a moving base,” *J. Vib. Control*, vol. 21, no. 6, pp. 1068–1085, 2015.

[27] U. H. Shah and K.-S. Hong, "Active vibration control of a flexible rod moving in water: Application to nuclear refueling machines," *Automatica*, vol. 93, pp. 231–243, 2018.

[28] K. Singh, S. Sharma, R. Kumar, and M. Talha, "Vibration control of cantilever beam using poling tuned piezoelectric actuator," *Mech. Based Des. Struct. Mach.*, vol. 51, no. 4, pp. 2217–2240, 2023.

[29] M. Cui, H. Liu, H. Jiang, Y. Zheng, X. Wang, and W. Liu, "Active vibration optimal control of piezoelectric cantilever beam with uncertainties," *Meas. Control*, vol. 55, no. 5–6, pp. 359–369, 2022.

[30] Z. Huang, F. Huang, X. Wang, and F. Chu, "Active vibration control of composite cantilever beams," *Materials*, vol. 16, no. 1, p. 95, 2022.

[31] Z. Qiu, Y. Yang, and X. Zhang, "Reinforcement learning vibration control of a multi-flexible beam coupling system," *Aerosp. Sci. Technol.*, vol. 129, p. 107801, 2022.

[32] Q. Lu, P. Wang, and C. Liu, "An analytical and experimental study on adaptive active vibration control of sandwich beam," *Int. J. Mech. Sci.*, vol. 232, p. 107634, 2022.

[33] K. G. Aktas and I. Esen, "State-space modeling and active vibration control of smart flexible cantilever beam with the use of finite element method," *Eng. Technol. Appl. Sci. Res.*, vol. 10, no. 6, pp. 6549–6556, 2020.

[34] X. Zhao, S. Zhang, Z. Liu, and Q. Li, "Vibration control for flexible manipulators with event-triggering mechanism and actuator failures," *IEEE Trans. Cybern.*, vol. 52, no. 8, pp. 7591–7601, 2021.

[35] M. Liu, D. Cao, J. Li, X. Zhang, and J. Wei, "Dynamic modeling and vibration control of a large flexible space truss," *Meccanica*, vol. 57, no. 5, pp. 1017–1033, 2022.

[36] M. Shao, Y. Huang, and V. V. Silberschmidt, "Intelligent manipulator with flexible link and joint: modeling and vibration control," *Shock Vib.*, vol. 2020, no. 1, p. 4671358, 2020.

[37] L. Cui, H. Wang, and W. Chen, "Trajectory planning of a spatial flexible manipulator for vibration suppression," *Robot. Auton. Syst.*, vol. 123, p. 103316, 2020.

[38] T. Long *et al.*, "A vibration control method for hybrid-structured flexible manipulator based on sliding mode control and reinforcement learning," *IEEE Trans. Neural Netw. Learn. Syst.*, vol. 32, no. 2, pp. 841–852, 2020.

[39] X. He, S. Zhang, Y. Ouyang, and Q. Fu, "Vibration control for a flexible single-link manipulator and its application," *IET Control Theory Appl.*, vol. 14, no. 7, pp. 930–938, 2020.

[40] J. Michael Sinapius *et al.*, "Active Vibration Control," in *Adaptronics–Smart Structures and Materials*, Springer, 2020, pp. 227–329.

[41] Q. Meng, X. Lai, Z. Yan, and M. Wu, "Tip position control and vibration suppression of a planar two-link rigid-flexible underactuated manipulator," *IEEE Trans. Cybern.*, vol. 52, no. 7, pp. 6771–6783, 2020.

[42] Q. Meng, X. Lai, Z. Yan, C.-Y. Su, and M. Wu, "Motion planning and adaptive neural tracking control of an uncertain two-link rigid–flexible manipulator with vibration amplitude constraint," *IEEE Trans. Neural Netw. Learn. Syst.*, vol. 33, no. 8, pp. 3814–3828, 2021.

[43] Z. Zhao, C. K. Ahn, and H.-X. Li, "Dead zone compensation and adaptive vibration control of uncertain spatial flexible riser systems," *IEEEASME Trans. Mechatron.*, vol. 25, no. 3, pp. 1398–1408, 2020.

[44] Z. Liu, X. He, Z. Zhao, C. K. Ahn, and H.-X. Li, "Vibration control for spatial aerial refueling hoses with bounded actuators," *IEEE Trans. Ind. Electron.*, vol. 68, no. 5, pp. 4209–4217, 2020.

[45] Q. C. Nguyen and H. Q. T. Ngo, "Input shaping control to reduce residual vibration of a flexible beam," *J. Comput. Sci. Cybern.*, vol. 32, no. 1, pp. 75–90, 2016.

[46] W. Singhose, "Command shaping for flexible systems: A review of the first 50 years," *Int. J. Precis. Eng. Manuf.*, vol. 10, pp. 153–168, 2009.

[47] D. K. Thomsen, R. Søe-Knudsen, O. Balling, and X. Zhang, "Vibration control of industrial robot arms by multi-mode time-varying input shaping," *Mech. Mach. Theory*, vol. 155, p. 104072, 2021.

[48] M. Kasprowiak, A. Parus, and M. Hoffmann, "Vibration suppression with use of input shaping control in machining," *Sensors*, vol. 22, no. 6, p. 2186, 2022.

[49] A. Mohammed, K. Alghanim, and M. Taheri Andani, "An adjustable zero vibration input shaping control scheme for overhead crane systems," *Shock Vib.*, vol. 2020, no. 1, p. 7879839, 2020.

[50] C. Ahumada and P. Wheeler, "Evaluation of input-shaping control robustness for the reduction of torsional vibrations," *IEEE Trans. Ind. Appl.*, vol. 57, no. 5, pp. 5028–5038, 2021.

[51] J. Wang, D.-X. Li, J. Wang, and D.-X. Li, "Optimal variable amplitudes input shaping control for slew maneuver of flexible spacecraft," *Rigid-Flex. Coupling Dyn. Control Flex. Spacecr. Time-Varying Parameters*, pp. 105–137, 2022.

[52] S. Bhattacharjee, J. J. Kim, and J. Hudson, "Input Shaping Control of a Flexible Structure for Rest-to-Rest and Non-Rest-to-Rest Maneuvers," *Appl. Sci.*, vol. 15, no. 6, p. 2952, 2025.

[53] W. Tang, R. Ma, W. Wang, and H. Gao, "Optimization-based input-shaping swing control of overhead cranes," *Appl. Sci.*, vol. 13, no. 17, p. 9637, 2023.

[54] S. Baklouti, E. Courteille, P. Lemoine, and S. Caro, "Input shaping for feed-forward control of cable-driven parallel robots," *J. Dyn. Syst. Meas. Control*, vol. 143, no. 2, p. 021007, 2021.

[55] A. B. Alhassan, R. Chancharoen, B. B. Muhammad, and G. Phanomchoeng, "Precise automation of rotary flexible link manipulator using hybrid input shaping with single state feedback fuzzy logic and sliding mode controllers," *IEEE Access*, vol. 11, pp. 86711–86726, 2023.

[56] W. Tang, E. Zhao, L. Sun, and H. Gao, "An active swing suppression control scheme of overhead cranes based on input shaping model predictive control," *Syst. Sci. Control Eng.*, vol. 11, no. 1, p. 2188401, 2023.

[57] G. Peláez, C. Alonso, H. Rubio, and J. C. García-Prada, "Performance analysis of input shaped model reference adaptive control for a single-link flexible manipulator," *J. Vib. Control*, vol. 30, no. 21–22, pp. 5018–5030, 2024.

[58] S. Y. S. Hussien, H. I. Jaafar, R. Ghazali, L. Ramli, and M. K. A. Johari, "Control of a Multimode Double-Pendulum Overhead Crane System Using Input Shaping Controllers.," *Int. J. Robot. Control Syst.*, vol. 4, no. 3, 2024.

[59] H.-P. Nguyen, N.-T. Bui, and others, "Tracking Control Based on Takagi-Sugeno Fuzzy Descriptor Model for Overhead Crane combined with Input Shaping," *IEEE Access*, 2024.

[60] M. F. Daqaq, C. Reddy, and A. H. Nayfeh, "Input-shaping control of nonlinear MEMS," *Nonlinear Dyn.*, vol. 54, pp. 167–179, 2008.

[61] K. Kim, J. Kim, Y. Park, S.-H. Kim, and J.-H. Lee, "Shaped input for reducing crosstalk of two-axis MEMS scanners," *Sens. Actuators Phys.*, vol. 349, p. 114002, 2023.

[62] T. D. Tuttle and W. P. Seering, "Experimental verification of vibration reduction in flexible spacecraft using input shaping," *J. Guid. Control Dyn.*, vol. 20, no. 4, pp. 658–664, 1997.

[63] U. H. Shah and K.-S. Hong, "Input shaping control of a nuclear power plant's fuel transport system," *Nonlinear Dyn.*, vol. 77, pp. 1737–1748, 2014.

[64] P.-T. Pham, G.-H. Kim, Q. C. Nguyen, and K.-S. Hong, "Control of a non-uniform flexible beam: Identification of first two modes," *Int. J. Control Autom. Syst.*, vol. 19, no. 11, pp. 3698–3707, 2021.

[65] M. Pant, H. Zaheer, L. Garcia-Hernandez, A. Abraham, and others, "Differential Evolution: A review of more than two decades of research," *Eng. Appl. Artif. Intell.*, vol. 90, p. 103479, 2020.

[66] T. A. Rahman, A. As'arry, N. A. Jalil, and R. Kamil, "Dynamic modelling of a flexible beam structure using feedforward neural networks for active vibration control," *Int. J. Automot. Mech. Eng.*, vol. 16, no. 1, pp. 6263–6280, 2019.

[67] W. Deng, S. Shang, X. Cai, H. Zhao, Y. Song, and J. Xu, "An improved differential evolution algorithm and its application in optimization problem," *Soft Comput.*, vol. 25, pp. 5277–5298, 2021.

[68] W. Deng, J. Xu, Y. Song, and H. Zhao, "Differential evolution algorithm with wavelet basis function and optimal mutation strategy for complex optimization problem," *Appl. Soft Comput.*, vol. 100, p. 106724, 2021.

[69] Y. Song, G. Zhao, B. Zhang, H. Chen, W. Deng, and W. Deng, "An enhanced distributed differential evolution algorithm for portfolio optimization problems," *Eng. Appl. Artif. Intell.*, vol. 121, p. 106004, 2023.

[70] T. N. Huynh, D. T. Do, and J. Lee, "Q-Learning-based parameter control in differential evolution for structural optimization," *Appl. Soft Comput.*, vol. 107, p. 107464, 2021.

[71] Z. Meng and C. Yang, “Two-stage differential evolution with novel parameter control,” *Inf. Sci.*, vol. 596, pp. 321–342, 2022.

[72] Y. Li, T. Han, S. Tang, C. Huang, H. Zhou, and Y. Wang, “An improved differential evolution by hybridizing with estimation-of-distribution algorithm,” *Inf. Sci.*, vol. 619, pp. 439–456, 2023.

[73] J. Sun, X. Liu, T. Bäck, and Z. Xu, “Learning adaptive differential evolution algorithm from optimization experiences by policy gradient,” *IEEE Trans. Evol. Comput.*, vol. 25, no. 4, pp. 666–680, 2021.

[74] G. Sun, B. Yang, Z. Yang, and G. Xu, “An adaptive differential evolution with combined strategy for global numerical optimization,” *Soft Comput.*, vol. 24, pp. 6277–6296, 2020.

[75] M. Georgioudakis and V. Plevris, “A comparative study of differential evolution variants in constrained structural optimization,” *Front. Built Environ.*, vol. 6, p. 102, 2020.

[76] Y. Han *et al.*, “Multi-strategy multi-objective differential evolutionary algorithm with reinforcement learning,” *Knowl.-Based Syst.*, vol. 277, p. 110801, 2023.

[77] E. Reyes-Davila, E. H. Haro, A. Casas-Ordaz, D. Oliva, and O. Avalos, “Differential evolution: a survey on their operators and variants,” *Arch. Comput. Methods Eng.*, vol. 32, no. 1, pp. 83–112, 2025.

[78] R. Storn and K. Price, “Differential evolution–a simple and efficient heuristic for global optimization over continuous spaces,” *J. Glob. Optim.*, vol. 11, pp. 341–359, 1997.

[79] C. Venkateswaran, M. Ramachandran, M. Amudha, T. Vennila, and M. Manjula, “A Review on Differential Evolution Optimization Techniques,” *Data Anal. Artif. Intell.*, vol. 1, no. 1, pp. 24–31, 2021.

[80] M. S. Saad, H. Jamaluddin, and I. Z. M. Darus, “Active vibration control of flexible beam using differential evolution optimisation,” *World Acad. Sci. Technol.*, vol. 6, no. 2, pp. 419–426, 2012.

[81] M. Marinaki, Y. Marinakis, and G. E. Stavroulakis, “Fuzzy control optimized by a multi-objective differential evolution algorithm for vibration suppression of smart structures,” *Comput. Struct.*, vol. 147, pp. 126–137, 2015.

[82] Y. Zhang, J. Liu, and W. He, “Vibration control for a nonlinear three-dimensional flexible manipulator trajectory tracking,” *Int. J. Control*, vol. 89, no. 8, pp. 1641–1663, 2016.

[83] M. Saad, “Evolutionary optimization and real-time self-tuning active vibration control of a flexible beam system,” *Ph Thesis Fac. Mech. Eng. Univ. Teknol. Malays.*, 2014.

[84] K. Nishihara and M. Nakata, “Comparison of adaptive differential evolution algorithms on the MOEA/D-DE framework,” in *2021 IEEE Congress on Evolutionary Computation (CEC)*, IEEE, 2021, pp. 161–168.

[85] S. M. Elsayed, R. A. Sarker, and D. L. Essam, “An improved self-adaptive differential evolution algorithm for optimization problems,” *IEEE Trans. Ind. Inform.*, vol. 9, no. 1, pp. 89–99, 2012.

[86] X. Zhang, L. Jin, C. Cui, and J. Sun, “A self-adaptive multi-objective dynamic differential evolution algorithm and its application in chemical engineering,” *Appl. Soft Comput.*, vol. 106, p. 107317, 2021.

[87] H. Zhang, J. Sun, K. C. Tan, and Z. Xu, “Learning adaptive differential evolution by natural evolution strategies,” *IEEE Trans. Emerg. Top. Comput. Intell.*, vol. 7, no. 3, pp. 872–886, 2022.

[88] Y. Cao and J. Luan, “A novel differential evolution algorithm with multi-population and elites regeneration,” *Plos One*, vol. 19, no. 4, p. e0302207, 2024.

[89] J.-S. Pan, N. Liu, and S.-C. Chu, “A hybrid differential evolution algorithm and its application in unmanned combat aerial vehicle path planning,” *IEEE Access*, vol. 8, pp. 17691–17712, 2020.

[90] J. Kushida, A. Hara, and T. Takahama, “Generation of adversarial examples using adaptive differential evolution,” *Int J Innov Comput Inf Control*, vol. 16, no. 1, pp. 405–414, 2020.

[91] S. Li, Q. Gu, W. Gong, and B. Ning, “An enhanced adaptive differential evolution algorithm for parameter extraction of photovoltaic models,” *Energy Convers. Manag.*, vol. 205, p. 112443, 2020.